Scientific Reports

https://doi.org/10.1038/s41598-026-43511-x

Article in Press

Quantitative assessment of apparent diffusion coefficient for neurological outcome prediction in status epilepticus: a pilot study

Received: 29 June 2025

Accepted: 4 March 2026

Published online: 19 March 2026

Cite this article as: Park S., Joo B., Kim T.J. *et al.* Quantitative assessment of apparent diffusion coefficient for neurological outcome prediction in status epilepticus: a pilot study. *Sci Rep* (2026). https://doi.org/10.1038/s41598-026-43511-x

Soo-Hyun Park, Byung-Euk Joo, Tae Jung Kim, Sang-Bae Ko, Kyungbok Lee, Dong-Eog Kim & Wi-Sun Ryu

Quantitative assessment of apparent diffusion coefficient for neurological outcome prediction in status epilepticus: a pilot study

Soo-Hyun Park[1*], Byung euk Joo[1], Tae Jung Kim MD, PhD[2,3], Sang-Bae Ko MD, PhD [2,3], Kyungbok Lee MD, PhD[1], Dong-Eog Kim MD, PhD[4], Wi-Sun Ryu MD, PhD[5*]

[1]Department of Neurology, Soonchunhyang University Seoul Hospital, Seoul, Korea

[2]Department of Neurology, Seoul National University College of Medicine, Seoul, Korea

[3]Department of Critical Care Medicine, Seoul National University Hospital, Seoul, Korea

[4]Department of Neurology, Dongguk University Hospital, Goyang, Korea

[5]JLK Inc., Seoul, South Korea

*These corresponding authors contributed equally to this work.

***Corresponding author**

Soo-Hyun Park, MD, PhD

Department of Neurology, Soonchunhyang University Seoul Hospital

59, Daesagwan-ro, Yongsan-gu, Seoul, Korea

Tel: +82-2-710-9538, E-Mail: g2skhome@gmail.com

Wi-Sun Ryu, MD, PhD

Artificial Intelligence R&D Center, JLK Inc.,

JLK TOWER, Teheran-ro 33-gil 5, Gangnam-gu, Seoul, Korea

Phone: +82-10-3574-6983; E-Mail: wisunryu@jlkgroup.com

Abstract

Status epilepticus (SE) is a neurological emergency with high morbidity and mortality. Early prognostication remains challenging, particularly in intensive care settings where clinical evaluations are limited. We investigated whether the voxel-wise proportion of preserved diffusion on diffusion-weighted imaging (DWI)—defined as the percentage of brain voxels with apparent diffusion coefficient (ADC) values between 600 and 1300 × 10^{-6} mm^2/s—may represent a potential imaging marker associated with clinical outcomes that warrants further validation. We retrospectively analyzed 59 patients with SE who underwent DWI and electroencephalography within 72 h of seizure onset. ADC quantification was performed using a fully automated, segmentation-free pipeline. Patients were stratified by tertiles and dichotomized using a receiver operating characteristic (ROC)-derived threshold. The primary outcome was defined as a good outcome, corresponding to no change or improvement of at least one point on the modified Rankin Scale from premorbid baseline to hospital discharge. Patients in the highest ADC tertile had significantly better outcomes (odds ratio [OR] 5.67, p = 0.024). At the optimal threshold of 0.797, preserved ADC was associated with favorable outcomes after adjustment for clinical variables (OR 6.05, p = 0.045),

along with younger age and lower EEG severity. A combined clinical–ADC model achieved an area under the ROC curve of 0.868. The preserved ADC was associated with improved outcome prediction and may provide exploratory imaging information for early risk assessment in patients with SE.

Keywords: Status epilepticus, diffusion-weighted imaging, apparent diffusion coefficient, outcome prediction, neurocritical care, artificial intelligence

Introduction

Status epilepticus (SE) constitutes a life-threatening neurological emergency with a considerable risk of long-term disability and mortality. Despite the therapeutic advancements, predicting neurological outcomes remain a complex and unresolved challenge for clinicians and caregivers alike[1]. Reliable early prognostic tools are essential for guiding the therapeutic intensity, rehabilitation planning, and discussions regarding care goals[2,3].

Several clinical factors have been consistently associated with the outcomes in SE, including etiology, age, baseline functional status, and electroencephalographic (EEG) features. Among these, etiology is regarded as one of the strongest determinants of prognosis, whereas advanced age and poor premorbid functional status are well-established predictors of unfavorable outcomes[4–7]. Specific EEG patterns, such as generalized periodic discharges, burst suppression, and lack of EEG reactivity have been consistently associated with a worse prognosis[8–10]. Although scoring systems such as the Status Epilepticus Severity Score (STESS)[11] and Epidemiology-Based Mortality Score in Status Epilepticus (EMSE)[8] provide structured prognostic frameworks, their predictive accuracy for individual patients remains limited, particularly during the early phase of SE (defined as within the first 24 h after seizure onset and before resolution of SE)[7].

The utility of clinical examination and EEG is often hampered by confounding factors such as sedation, neuromuscular blockade use, or altered consciousness in the intensive care unit (ICU). Furthermore, EEG interpretation requires specialist expertise and may not be consistently available in real time. These challenges underscore the need for an automated, objective imaging biomarker that can facilitate early risk stratification independent of patient responsiveness

and specialist availability.

Neuroimaging, particularly diffusion-weighted imaging (DWI) and apparent diffusion coefficient (ADC) maps, has emerged as a key tool for evaluating the brain injury in SE and related conditions[8–10]. Previous studies have largely relied on qualitative assessments or region-of-interest (ROI)–based measurements to characterize peri-ictal magnetic resonance imaging abnormalities (PMA)[7,12,13]. Recently, quantitative approaches to DWI/ADC analysis in SE have been reported, with proposed cutoff values for prognostication[14]. However, these methods are limited by regional sampling and the lack of whole-brain representation.

To overcome these limitations, we applied a fully segmentation-free, voxel-wise analysis of ADC distribution across the entire brain. This automated approach enables an objective and highly reproducible quantification of the proportion of brain tissue with preserved diffusion, eliminating observer bias and allowing for rapid assessment without manual intervention. We hypothesized that a higher whole-brain normal ADC ratio would be associated with favorable neurological outcomes in patients with SE. Accordingly, this study aimed to evaluate the relationship between diffusion preservation and functional recovery and assess the clinical utility of this metric as a simple and scalable imaging biomarker for outcome prediction in SE.

Results

Clinical characteristics

Overall, 59 patients with SE were included in the analysis (age, 60.3±17.6, mean ± standard deviation [SD]; male, 67.8%), comprising 39 patients with good outcomes and 20 with poor outcomes. The clinical outcomes were categorized

based on changes in the modified Rankin Scale (mRS) from the premorbid state to hospital discharge. A good outcome was defined as no change or an improvement of at least one point on the mRS, whereas a poor outcome was defined as a deterioration of at least one point. Patients in the poor outcome group were significantly older than those in the good outcome group (68.8 ± 16.4 vs. 55.9 ± 16.7 years, $p = 0.007$). No significant differences were observed between the groups in terms of premorbid mRS score, sex, or major vascular comorbidities (Table 1).

The EEG patterns differed significantly between the outcome groups ($p = 0.022$), with patients with poor outcomes more frequently exhibiting epileptiform activity, whereas patients with good outcomes more commonly showed no abnormalities or diffuse slowing. Admission Glasgow Coma Scale (GCS) scores were significantly lower in the poor outcome group than in the good outcome group (median [interquartile range, IQR]: 8.0 [5.0–12.3] vs. 11.0 [8.0–13.0], $p = 0.027$). SE semiology showed a trend toward association with outcome, but did not reach statistical significance ($p = 0.072$). The etiological categories were not significantly associated with the outcome ($p = 0.294$).

The duration of clinical symptoms was numerically longer in the poor outcome group (139.2 ± 240.8 min, mean ± SD) than in the good outcome group (59.3 ± 70.5 min, mean ± SD), although this difference was not statistically significant ($p = 0.058$).

Patients with poor outcomes had a significantly longer ICU length of stay than those with good outcomes (median [IQR], 30.5 [15.8–51.3] vs. 7 [3–15] days; $p < 0.001$).

MRI acquisition timing and potential confounding

The interval from seizure onset to MRI acquisition was quantified to assess the potential confounding effects of imaging timing on ADC measurements. The median time to MRI was 6.48 h (IQR, 3.52–13.83) in the good outcome group and 6.10 h (IQR, 4.43–13.43) in the poor outcome group, with no significant difference between groups ($p = 0.899$, Table 1). Sensitivity analyses using a 6-h threshold further corroborated that the acquisition timing did not substantially bias our prognostic inferences (Table 2). Following adjustment for this temporal latency, the independent association between the normal ADC ratio and clinical recovery remained materially unchanged ($p = 0.955$, Table 3).

Quantitative ADC analysis and normal ADC ratio tertile analysis

A quantitative voxel-wise ADC analysis revealed that the proportion of brain voxels within the normal ADC range (600–1300×10^{-6} mm^2/s) was significantly higher in the good outcome group (81.0 ± 5.5, mean ± SD, %) than in the poor outcome group (75.9 ± 6.6, mean ± SD, %, $p = 0.003$, Table 1). As shown in Fig. 1, voxel-wise ADC distributions in the good outcome group showed a narrow, symmetrical peak centered within the normal range, whereas the poor outcome group exhibited a broader and more right-shifted distribution, suggesting increased high-range ADC values.

To further evaluate the prognostic relevance of diffusion preservation, the patients were stratified into tertiles based on their individual normal ADC ratios: Tertile 1 (low: 0.623–0.766), Tertile 2 (intermediate: 0.767–0.818), and Tertile 3 (high: 0.819–0.902; Supplementary Table S1, Fig. 2). The mean normal ADC ratio increased progressively across groups: 0.723 ± 0.033 in low, 0.794 ± 0.016 in

intermediate, and 0.861 ± 0.028 in high. A corresponding trend in good outcome rates was observed (50.0%, 63.2 %, and 85.0% in the low-, intermediate-, and high groups, respectively; $p = 0.062$, Supplementary Table S1, Fig. 3). Univariate logistic regression confirmed this relationship: patients in the highest tertile had significantly greater odds of good outcome (odds ratio [OR] 5.67, 95% confidence intervals [CI] 1.25–25.61, $p = 0.024$) than those in the lowest tertile, whereas the intermediate group showed no significant difference (OR 1.71, 95% CI 0.48–6.16, $p = 0.409$, Table 2). These findings suggest a nonlinear trend in the outcome probability across ADC tertiles, prompting further analysis to determine a clinically actionable threshold.

Voxel-wise DWI/ADC group classification and outcome association

The distribution of ADC values exhibited distinct histogram patterns across the three groups, with the DWI hyperintensity with low ADC showing a prominent leftward skew and DWI hyperintensity with high ADC demonstrating a rightward shift (Supplementary Fig. S1). Upon visual inspection of the DWI and corresponding ADC maps, 34 patients (57.6%) showed no DWI hyperintensity, 18 patients (30.5%) exhibited DWI hyperintensity with low ADC, and 7 patients (11.9%) demonstrated DWI hyperintensity with high ADC. Accordingly, ADC abnormalities were observed as decreased ADC in 18 patients (30.5%) and increased ADC in 7 patients (11.9%), whereas 34 patients (57.6%) had no visually apparent diffusion abnormality (Supplementary Table S2).

Although the median GCS scores and sedation rates were comparable across these groups (Supplementary Table S2), the clinical outcomes differed markedly. Good outcome rates were high in both no DWI hyperintensity (85.3%) and DWI

hyperintensity with high ADC (85.7%); however, only 22.2% of patients with DWI hyperintensity with low ADC achieved a good outcome ($p < 0.001$). The ICU length of stay differed across the DWI/ADC voxel groups, with the longest ICU length of stay observed in patients with DWI hyperintensity and low ADC (median [IQR], 17.5 [12.25–33.0] days) compared with those without DWI hyperintensity (9.5 [3.25–20.0] days) or with DWI hyperintensity and high ADC (11.0 [5.0–18.0] days), although this difference did not reach significance ($p = 0.060$).

ROC-based cut-off derivation and clinical application

Receiver operating characteristic curve (ROC) analysis identified an optimal threshold of 0.797 for the normal ADC ratio, yielding an area under the ROC (AUROC) of 0.732, with 64.1% sensitivity, 85.0% specificity, 89.3% positive predictive value (PPV), 54.8% negative predictive value (NPV), and an overall accuracy of 71.2%. This threshold was used to dichotomize the patients into "Preserved ADC" (≥ 0.797) and "Non-preserved ADC" (< 0.797) groups.

In a multivariable logistic regression model adjusted for age, premorbid mRS, and EEG severity, a normal ADC ratio ≥ 0.797 (Preserved ADC group) was independently associated with good outcomes (OR 6.05, 95% CI 1.04–35.09, $p = 0.045$). The other independent predictors included younger age (OR per year increase: 0.95, $p = 0.047$), lower EEG severity (OR for moderate vs. severe: 0.33, $p = 0.015$), and lower premorbid disability (OR per point increase in pre-mRS: 1.88, $p = 0.047$; Table 3).

Prognostic performance comparison

The prognostic performance of models using continuous versus dichotomized

ADC ratios was compared using an ROC analysis. The ADC-only model with continuous ADC yielded an AUROC of 0.732, whereas the clinical-only model (age, premorbid mRS, and EEG severity) achieved an AUROC of 0.829, and the combined model integrating continuous ADC and clinical features showed an AUROC of 0.860 (Fig. 4A). When the normal ADC ratio was dichotomized at the 0.797 cut-off, the cutoff-based ADC-only model achieved an AUROC of 0.746, and the combined model with dichotomized ADC and clinical variables reached an AUROC of 0.868 (Fig. 4B). Although incorporation of either continuous or dichotomized ADC ratio numerically increased the AUROC compared to the clinical-only model (0.860 vs. 0.829 and 0.868 vs. 0.829, respectively), these exploratory improvements did not reach statistical significance (continuous ADC: $p = 0.933$; dichotomized ADC: $p = 0.394$). The established bedside severity scores demonstrated moderate prognostic performance (STESS AUROC 0.722; mSTESS AUROC 0.694, Supplementary Table 3).

Discussion

In this exploratory pilot study, we observed that the proportion of brain voxels within the normal ADC range is independently associated with the clinical outcomes in patients with SE. Using a fully automated, voxel-wise segmentation approach, we introduced the normal ADC ratio as a quantitative global imaging metric of diffusion integrity. We identified a potential clinically relevant threshold: patients with a normal ADC ratio ≥79.7%, defined as the "Preserved ADC group," had demonstrated significantly higher odds of favorable outcomes compared with that in the "Non-preserved ADC group" (<79.7%). The preserved ADC can be extracted from routine DWI without manual ROI placement, enabling reproducible and operator-independent quantification.

In the ICU setting, clinical examination and EEG assessment may be constrained by several practical factors, including limited access to continuous EEG monitoring, delays in expert interpretation, and technical challenges related to sedation, motion artifacts, and altered levels of consciousness[9,10,15]. These limitations highlight the potential value of objective, automated imaging biomarkers that can support early prognostication, independent of patient responsiveness or specialist availability. The preserved ADC may serve as a candidate imaging metric for future studies investigating imaging-based prognostic assessment strategies. With minimal post-processing, the preserved/non-preserved ADC status may be incorporated into radiologic workflows or clinical dashboards to complement early risk stratification.

The prognostic relevance of ADC is rooted in the pathophysiology of SE. Prolonged seizure activity leads to excessive glutamate release, resulting in an excitotoxic calcium influx, mitochondrial dysfunction, and ATP depletion[16,17]. This disrupts the Na^+/K^+ ATPase function, leading to intracellular sodium and water accumulation and ultimately cytotoxic edema, which restricts extracellular water diffusion and low ADC values[16-18]. Therefore, the preserved ADC reflects intact cellular energy metabolism and membrane integrity, indicating that widespread irreversible injury has not yet occurred[17]. Thus, a high normal ADC ratio may signify a potentially reversible stage of injury, where functional recovery remains possible.

To further elucidate the prognostic significance of voxel-level ADC patterns, we stratified patients based on the presence of DWI hyperintensity and ADC directionality. The outcome differences among these groups were notable, whereas patients with DWI hyperintensity and high ADC exhibited a similar rate of favorable recovery compared to those without DWI hyperintensity (85.3% and

85.7%, respectively), only 22.2% of patients with DWI hyperintensity and low ADC achieved good outcomes. In addition, to address the potential confounding effects of motion artifacts, especially in critically ill patients, we examined the sedation status and GCS at the time of imaging, which did not differ across the groups. These findings suggest that the observed diffusion patterns likely reflect the underlying tissue physiology rather than imaging artifacts.

Although most previous studies have focused on ADC reduction as a marker of cytotoxic edema, our study highlights the clinical significance of elevated ADC values in patients with SE. Patients with DWI hyperintensity and high ADC showed favorable outcomes comparable to those without DWI hyperintensity. This finding indicates that DWI hyperintensity accompanied by a high ADC may reflect reversible, non-cytotoxic processes such as vasogenic edema, reactive hyperperfusion, or transient postictal shifts in diffusion dynamics[20-22]. These findings expand upon prior studies on SE, traumatic brain injury, hypoxic–ischemic encephalopathy, and cardiac arrest, which have shown associations between low ADC and poor outcomes[23-25].

Despite the well-established influence of the underlying etiology on the outcomes of SE, etiological categories were not significantly associated with the outcomes in our cohort. Moreover, the prognostic performance of ADC-derived metrics remained robust after adjusting clinical variables, including etiology, EEG patterns, level of consciousness, and seizure semiology. These findings suggest that whole-brain voxel-based ADC analysis provides prognostic information that is not solely driven by the underlying etiology. Furthermore, a potential overlap between PMA and diffusion changes caused by acute structural lesions is mitigated by whole-brain voxel-based ADC analysis, which emphasizes global diffusion distributions rather than localized abnormalities.

Several clinical prognostic scores have been proposed for SE, including STESS[11], its modified version (mSTESS)[6], EMSE[8], and the END-IT score[25]. Although these tools provide structured clinical frameworks, their application in acute ICU settings may be limited by incomplete clinical information, delayed availability of key components, and inter-observer variability. In our cohort, established bedside scores demonstrated moderate prognostic performance (STESS AUROC 0.722; mSTESS AUROC 0.694), comparable to the ADC-only model (AUROC 0.732). Integrating quantitative ADC metrics with clinical variables numerically improved discrimination compared with the clinical models alone, although these differences did not reach statistical significance. These findings suggest that automated whole-brain ADC analysis offers complementary prognostic information beyond traditional bedside assessments and may help bridge the gap between readily available clinical scores and objective neuroimaging biomarkers in critically ill patients with SE.

In the context of prior imaging-based studies, diffusion abnormalities in SE have predominantly been evaluated using qualitative assessment or regional ROI-based ADC measurements.[12,13] Quantitative analyses have shown that regional ADC reduction is associated with clinical outcomes, with reported imaging-based AUROC values around 0.70.[14] Other MRI studies focusing on peri-ictal abnormalities have similarly demonstrated modest discriminative performance, generally ranging between 0.65 and 0.75 when imaging variables were analyzed alone.[12,13] In comparison, the standalone normal ADC ratio in our cohort achieved an AUROC of 0.732, which falls within the range of previously reported diffusion-based approaches. When integrated with clinical severity variables, the combined model reached an AUROC of 0.868. Although direct head-to-head comparisons were not performed and external validation is required, these findings position

automated whole-brain ADC quantification as a standardized and reproducible approach compared with regional ROI-based strategies.

Against this backdrop, automated imaging-based biomarkers may offer complementary value by providing objective and readily available prognostic information. This study highlights the potential of an automated, artificial intelligence (AI)-assisted imaging analysis for outcome prediction in neurocritical care[26-28]. The preserved ADC was computed using a voxel-wise, ROI-free segmentation pipeline, allowing for a reproducible quantification of global diffusion characteristics without manual input[29]. This approach reduces inter-observer variability and facilitates rapid whole-brain ADC histogram analysis. As the neuroimaging data volume and complexity continue to grow, the integration of AI-driven analytical methods will be essential for developing scalable, real-time prognostic tools.

From a clinical implementation perspective, voxel-wise continuous ADC ratio modeling provides detailed prognostic information but may be limited by its complexity and interpretability in routine settings. Application of a simplified dichotomized threshold (≥0.797) yielded comparable predictive performance when combined with clinical parameters, without substantial loss of discrimination. This suggests that a clinically practical cutoff can serve as a practical surrogate for more complex quantitative metrics in real-world decision-making.

Despite the pathophysiological insights provided by quantitative neuroimaging, obtaining acute DWI/ADC MRI remains challenging in critically ill patients, as MRI acquisition is resource-dependent and often delayed by logistical constraints, in contrast to bedside clinical scoring systems. Prior studies have demonstrated that PMA evolve dynamically over time and are influenced by imaging timing,

underscoring the potential impact of delayed acquisition on ADC measurements[30-33]. To address this concern, we explicitly quantified the interval from seizure onset to MRI and incorporated the imaging delay into our multivariable analyses. Although adjustment for imaging delay did not materially alter the associations observed in our cohort, standardized imaging protocols would further enhance consistency. These findings underscore the complementary role of quantitative neuroimaging alongside clinically accessible bedside assessments.

Several limitations should be acknowledged. First, this was a single-center retrospective pilot study with a relatively small sample size, and the findings should therefore be considered hypothesis-generating rather than confirmatory. Larger prospective multicenter cohorts are required to validate the robustness of the observed associations. Second, although our results were interpreted in relation to previously published imaging-based prognostic studies, we did not perform direct head-to-head comparisons within the same cohort using alternative ROI-based ADC methods or previously established imaging models. Accordingly, the incremental value of whole-brain voxel-wise quantification over regional approaches remains to be confirmed in future comparative investigations. In addition, the ROC-derived cutoff (0.797) was identified and evaluated within the same dataset without external validation. This may introduce optimism bias and limit generalizability across different scanners, acquisition protocols, and patient populations. Furthermore, although the combined model numerically improved discriminative performance compared with clinical variables alone, the differences in AUROC did not reach statistical significance and should therefore be interpreted cautiously. Third, MRI acquisition timing varied between patients, and although adjustment for imaging

delay did not materially alter the associations observed, standardized imaging protocols would enhance consistency. Clinical outcomes were assessed at hospital discharge rather than at longer-term follow-up, and continuous EEG monitoring was not routinely available. The cohort was heterogeneous with respect to etiology, seizure duration, and treatment intensity, and additional unmeasured confounders—including sedative exposure and dynamic EEG evolution—may have influenced outcome classification. Finally, while the voxel histogram analysis was automated and reproducible within our platform, its robustness across diverse imaging environments and the potential impact of anatomical distribution of preserved ADC warrant further investigation.

Conclusion

This exploratory study suggests that the normal ADC ratio may represent a quantitative automated imaging metric associated with clinical outcomes in SE. Using a voxel-wise analysis of routine diffusion-weighted MRI, we identified a potential clinically relevant threshold of 79.7%, which was associated with a more than sixfold increase in the likelihood of favorable outcomes. This marker can be obtained without manual segmentation and may provide imaging information complementary to established clinical predictors.

Methods

Study design and population

This retrospective study initially identified 94 consecutive adult patients diagnosed with SE who underwent brain MRI, including DWI and EEG, between

January 2021 and January 2025. SE was defined according to the ILAE criteria, which specify either continuous seizure activity lasting longer than 5 min or two or more seizures without full recovery between episodes. Only patients managed in the neurological ICU with available clinical, EEG, and imaging data were screened. Patients were excluded if they were younger than 19 years (n = 7), had a premorbid mRS score of 5 (n = 12), or lacked DWI at the time of evaluation (n = 16). These criteria were applied to ensure cohort homogeneity and exclude cases with uniformly unfavorable baseline functional statuses that might introduce selection bias. After these exclusions, 59 patients were included in the final analysis. The patient selection process is summarized in Supplementary Fig. S2.

Clinical and imaging data collection

The clinical data collected for each patient included age, pre-mRS, and comorbidities documented in the medical records. Neurological assessments were performed for clinical outcome evaluation during ICU hospitalization by trained medical staff. The level of consciousness at presentation was assessed using the GCS[34].

SE semiology was classified as convulsive or non-convulsive based on clinical documentation and EEG findings[35]. EEG recordings were acquired using the standard 10–20 electrode placement system with bipolar and referential montages, following the guidelines of the American Clinical Neurophysiology Society[2]. The original EEG interpretations and reports were generated by two experienced neurologists. The EEG severity was scored using a simplified ordinal scale as follows: no abnormality, mild abnormality, moderate abnormality, and

severe abnormality[3]. For descriptive analyses, the EEG pattern categories were as follows: no abnormality, diffuse slowing, rhythmic or focal slowing with sharp waves, and epileptiform activity[9,10]. Etiology was classified according to the ILAE framework into acute symptomatic (structural, metabolic/toxic, or infectious), remote symptomatic (remote structural), progressive, and unknown causes based on clinical, laboratory, and neuroimaging data[3].

All EEG and clinical evaluations were performed according to standard protocols, and the recordings were interpreted by experienced neurologists.

MRI acquisition timing and adjustment for imaging delay

Brain MRI, including DWI and ADC sequences, was performed during acute hospitalization according to clinical stability and logistical availability, typically within 72 h after seizure onset. Given the potential influence of imaging timing on ADC measurements, as PMA are known to evolve dynamically over time in SE[30-33], we quantified the interval from seizure onset to MRI acquisition for each patient. For cases in which imaging occurred after midnight relative to symptom onset, timing was automatically adjusted to account for day transitions. MRI delay was expressed in hours and was primarily analyzed as a continuous variable. Differences in the MRI delay between outcome groups were assessed using the Mann–Whitney U test. To address the potential confounding, an MRI delay was included as a covariate in multivariable models examining the association between ADC-derived metrics and clinical outcomes. In exploratory analyses, a pragmatic binary threshold (>6 vs. ≤6 h) was applied to facilitate clinical interpretation.

Voxel-wise ADC quantification and normal ADC ratio derivation

Voxel-wise ADC values were extracted from whole-brain DWI images using a fully automated, proprietary, ROI-free method to eliminate the potential observer bias and ensure maximal reproducibility and standardization across all subjects. Instead of limiting the analysis to predefined regions, the entire brain volume was comprehensively analyzed to maintain objectivity and avoid user-dependent variability[4]. This whole-brain, segmentation-free approach enabled standardized, reproducible assessment of diffusion abnormalities across patients. Automated diffusion analysis was performed using a validated AI-assisted neuroimaging platform (JLW DWI, JLK Inc., Seoul, South Korea)[29,36] that integrates brain extraction, normalization, and voxel-wise ADC quantification based on standardized brain parcellation (Supplementary Fig. S3).

The voxel counts across the full ADC spectrum (200–1950 $\times 10^{-6}$ mm²/s) were quantified. For each patient, the normal ADC ratio was defined as the proportion of brain voxels with ADC values within the physiologically preserved range (600–1300 $\times 10^{-6}$ mm²/s) relative to the total number of brain voxels. Each voxel was further categorized as low ADC (<600 $\times 10^{-6}$ mm²/s), normal ADC (600–1300 $\times 10^{-6}$ mm²/s), or high ADC (>1300 $\times 10^{-6}$ mm²/s)[14,15,37,38].

To minimize the contamination from focal structural lesions such as acute ischemic stroke or encephalitis, DWI/ADC maps were visually reviewed in conjunction with conventional MRI sequences and clinical information, and voxels showing clear vascular territorial patterns consistent with acute structural lesions were excluded from classification. Peri-ictal changes were defined as non-territorial or bilateral diffusion abnormalities. This whole-brain voxel-based approach reduces the influence of focal etiological lesions on the global ADC metrics. Representative patient examples illustrating voxel-wise DWI/ADC

analysis are shown in Supplementary Fig. S3.

Stratification and outcome definition

To examine the association between diffusion preservation and clinical outcomes, the patients were stratified into tertiles based on their individual normal ADC ratio. The cut-off values for Tertile 1 (low), Tertile 2 (intermediate), and Tertile 3 (high) were determined using the 33.3rd and 66.6th percentiles of the normal ADC ratio distribution, allowing for a grouping approach based on relative distribution within the cohort rather than absolute thresholds.

In addition, patients were classified into three groups based on a voxel-wise analysis of DWI and the corresponding ADC values to further characterize the prognostic implications of diffusion abnormalities. DWI hyperintense lesions were automatically segmented using threshold-based extraction, and the ADC values in these regions were analyzed. The patients were categorized as follows: 1) no DWI hyperintensity, 2) DWI hyperintensity with low ADC ($<600 \times 10^{-6}$ mm^2/s), and 3) DWI hyperintensity with high ADC ($>1300 \times 10^{-6}$ mm^2/s).

Clinical outcomes were defined based on the mRS change from the premorbid state to discharge. A good outcome was defined as no change or improvement of at least one point in mRS, whereas a poor outcome was defined as a deterioration of at least one point[39,40].

The STESS and mSTESS were calculated according to the published definitions[6,11]. STESS incorporates age, level of consciousness, seizure type, and history of epilepsy. An age ≥ 65 years was assigned 2 points. The level of consciousness was approximated using the GCS, with a GCS score of ≤ 8 considered equivalent to stupor/coma (1 point). The seizure type was derived

from SE semiology and GCS, with convulsive SE assigned 1 point, nonconvulsive SE with coma (GCS ≤ 8) assigned 2 points, and nonconvulsive SE without coma assigned 0 points. An absence of prior epilepsy was assigned 1 point.

The mSTESS was calculated using the same components, with an age threshold of ≥ 70 years and additional weighting for premorbid functional status. Premorbid mRS was categorized as 0 (0 points), 1–3 (1 point), and > 3 (2 points), consistent with prior reports.

Statistical Analysis

Continuous variables were presented as mean ± SD or median (IQR) and were compared using the independent t-test, Mann–Whitney U test, or Kruskal–Wallis test as appropriate, with post-hoc pairwise testing where applicable.

To evaluate the prognostic performance, the normal ADC ratio was used as both a continuous and categorical variables (based on empirically derived tertiles or ROC-derived cut-offs). Univariate and multivariable logistic regression models were constructed to evaluate the association between the ADC-based measures and clinical outcomes. Candidate variables with $p < 0.2$ in univariate analysis were entered into the multivariable model to ensure the inclusion of potentially relevant predictors. All models were adjusted for relevant clinical covariates. OR, 95% CI, and p-values were reported.

AUROC was used to compare the model's performance. AUROC analysis was used to identify the optimal cutoff value via the Youden Index. To compare AUROCs between models, DeLong's test for two correlated AUROC curves was applied. Diagnostic metrics—including sensitivity, specificity, PPV, NPV, and accuracy—were computed.

Statistical significance was defined as $p < 0.05$. All statistical analyses were conducted using SPSS version 26.0 for Windows (SPSS Inc., Chicago, IL, USA), and graphical data analysis was conducted using R version 4.0.1 (Washington University, St. Louis, MO, USA).

Because this study was designed as an exploratory retrospective imaging analysis, no formal a priori sample-size calculation was performed, which is consistent with hypothesis-generating imaging studies. The study population was determined by consecutive eligible patients during the predefined study period.

References

1. Riney K, et al. International League Against Epilepsy classification and definition of epilepsy syndromes with onset at a variable age: Position statement by the ILAE Task Force on Nosology and Definitions. Epilepsia. 63, 1443–1474 (2022).

2. Guérit JM, et al. Consensus on the use of neurophysiological tests in the intensive care unit (ICU): Electroencephalogram (EEG), evoked potentials (EP), and electroneuromyography (ENMG). Neurophysiol Clin. 39, 71–83 (2009).

3. Centorrino F, et al. EEG abnormalities during treatment with typical and atypical antipsychotics. Am J Psychiatry. 159, 109–115 (2002).

4. Oishi K, et al. Quantitative evaluation of brain development using anatomical MRI and diffusion tensor imaging. Int J Dev Neurosci. 31, 512–524 (2013).

5. Sener RN. Diffusion MRI: Apparent diffusion coefficient (ADC) values in the normal brain and a classification of brain disorders based on ADC values. Comput Med Imaging Graph. 25, 299–326 (2001).

6. Sutter R, Kaplan PW, Rüegg S. Outcome predictors for status epilepticus—what really counts. Nat Rev Neurol. 9, 525–534 (2013).

7. Neligan A, Shorvon SD. Prognostic factors, morbidity and mortality in tonic–clonic status epilepticus: A review. Epilepsy Res. 93, 1–10 (2011).

8. Leitinger M, et al. Epidemiology-based mortality score in status epilepticus (EMSE). Epilepsia 56, 198–208 (2015).

9. Hirsch LJ, et al. American Clinical Neurophysiology Society's standardized critical care EEG terminology: 2012 version. J Clin Neurophysiol. 30, 1–27 (2013).

10. Azabou E, et al. Value and mechanisms of EEG reactivity in the prognosis of patients with impaired consciousness: a systematic review. Crit Care. 22, 184 (2018).

11. Rossetti AO, Hurwitz S, Logroscino G, Bromfield EB. Prognosis of status epilepticus: Role of aetiology, age, and consciousness impairment at presentation. J Neurol Neurosurg Psychiatry. 77, 611–615 (2006).

12. Bosque Varela P, et al. Imaging of status epilepticus: Making the invisible visible. A prospective study on 206 patients. Epilepsy Behav. 141,109130 (2023).

13. Giovannini G, Kuchukhidze G, McCoy MR, Meletti S, Trinka E. Neuroimaging alterations related to status epilepticus in an adult population: Definition of MRI findings and clinical-EEG correlation. Epilepsia. 59,120-127 (2018).

14. Machegger L, et al. Quantitative analysis of diffusion-weighted imaging and apparent diffusion coefficient in status epilepticus and acute ischemic stroke. Front Neurol. 13, 905457 (2022).

15. Sutter R, Stevens RD, Kaplan PW. Continuous electroencephalographic monitoring in critically ill patients: Indications, limitations, and strategies. Critical care medicine. 41, 1124-1132 (2013).

16. Kim JA, et al. Transient MR signal changes in patients with generalized tonic-clonic seizure or status epilepticus: Periictal diffusion-weighted imaging. AJNR Am J Neuroradiol. 22, 1149–1160 (2001).

17. Kassem-Moussa H, Provenzale JM, Petrella JR, Lewis DV. Early diffusion-weighted MR imaging abnormalities in sustained seizure activity. AJR Am J Roentgenol. 174, 1304–1306 (2000).

18. Zhao M, et al. Mitochondrion-based organellar therapies for central nervous system diseases. Cell Commun Signal. 22, 487 (2024).

19. Xie W, et al. Unraveling the nexus of age, epilepsy, and mitochondria. Front Pharmacol. 15, 1469053 (2024).

20. Koch S, Rabinstein A, Falcone S, Forteza A. Diffusion-weighted imaging shows cytotoxic and vasogenic edema in eclampsia. AJNR Am J Neuroradiol. 22, 1068–1070 (2001).

21. Hasegawa Y, Fisher M, Latour LL, Dardzinski BJ, Sotak CH. MRI diffusion mapping of reversible and irreversible ischemic injury. Neurology. 44, 1484–1490 (1994).

22. Meyer M, Juenemann M, Braun T, Schirotzek I, Schramm P. Intact cerebrovascular autoregulation in refractory status epilepticus. Crit Care. 23, 6

(2019).

23. Diamanti S, et al. Prognostic value of MRI abnormalities in post-anoxic super-refractory status epilepticus. Eur J Neurol. 32, e70045 (2025).

24. Calabrese E, et al. Parieto-occipital injury on diffusion MRI correlates with outcome after cardiac arrest. AJNR Am J Neuroradiol. 44, 254–260 (2023).

25. Gao Q, et al. Prediction of functional outcome in patients with convulsive status epilepticus: the END-IT score. Crit Care. 20, 46 (2016).

26. Kawai Y, et al. Explainable artificial intelligence-based prediction of poor neurological outcome from head computed tomography in the immediate post-resuscitation phase. Sci Rep**.** 13, 5759 (2023).

27. Vitt JR, Mainali S. Artificial Intelligence and Machine Learning Applications in Critically Ill Brain Injured Patients. Semin Neurol. 44, 342–356 (2024).

28. Badjatia N, et al. Machine Learning Approaches to Prognostication in Traumatic Brain Injury. Curr Neurol Neurosci Rep. 25, 19 (2025).

29. Ryu WS. et al. Acute Infarct Segmentation on Diffusion-Weighted Imaging Using Deep Learning Algorithm and RAPID MRI. J Stroke. 25, 425–429 (2023).

30. Di Bonaventura C, et al. Diffusion-weighted magnetic resonance imaging in patients with partial status epilepticus. Epilepsia. 50 Suppl 1, 45-52 (2009).

31. Huang YC, et al. Periictal magnetic resonance imaging in status epilepticus. Epilepsy Res. 86, 72–81 (2009).

32. Köstner M, et al. Large-scale transient peri-ictal perfusion magnetic resonance imaging abnormalities detected by quantitative image analysis. Brain Commun. 24, fcad047 (2023).

33. Wieshmann UC, Symms MR, Shorvon SD. Diffusion changes in status epilepticus. Lancet 350, 493–494 (1997).

34. Husain AM. Electroencephalographic assessment of coma. J Clin Neurophysiol. 23, 208-220 (2006).

35. Trinka E, et al. A definition and classification of status epilepticus--Report of the ILAE Task Force on Classification of Status Epilepticus. Epilepsia. 56, 1515–1523 (2015).

36. Ryu WS, et al. Deep learning-based automatic infarct segmentation. Sci Rep. 15, 13214 (2025).

37. Annet L, et al. Apparent diffusion coefficient measurements within intracranial epidermoid cysts in six patients. Neuroradiology 44, 326–328 (2002).

38. Hilario A, et al. The added value of apparent diffusion coefficient to cerebral blood volume in the preoperative grading of diffuse gliomas. AJNR Am J Neuroradiol. 33, 701–707 (2012).

39. Saver JL, et al. Standardized Nomenclature for Modified Rankin Scale Global Disability Outcomes: Consensus Recommendations From Stroke Therapy Academic Industry Roundtable XI. Stroke. 52, 3054–3062 (2021).

40. Seker F, et al. Clinical Outcome after Thrombectomy in Patients with Stroke with Premorbid Modified Rankin Scale Scores of 3 and 4: A Cohort Study with 136 Patients. AJNR Am J Neuroradiol. 40, 283–286 (2019).

Authors' contributions

SHP and WSR conceived and designed the study. BEJ and KBL collected and verified the data. SHP, TJK, SBK, DEK and WSR did the statistical analysis. SHP

and WSR interpreted the data. All authors critically revised the manuscript for important intellectual content and agreed to submit the final version for publication. We confirm that the manuscript complies with all instructions to authors.

Funding

This research was supported by Soonchunhyang University. The funders had no role in the design of the study; the collection, analysis, and interpretation of data; the writing of the manuscript; or the decision to submit it for publication.

Declarations

Ethics approval and consent to participate

This study was conducted following the principles outlined in the Declaration of Helsinki. This study was approved by the Institutional Review Board of Soonchunhyang University Hospital Seoul (IRB No. SCHUH 2025-02-007), and the requirement for informed consent was waived due to the retrospective nature of the study.

Data availability statement

The data that supports the findings of this study are available from the corresponding author upon reasonable request.

Competing interests

The authors declare no competing interests

Code availability

The computational framework of this study, comprising the R scripts for voxel-wise modeling and anonymized datasets necessary for replication, is publicly

available via GitHub [https://github.com/g2skhome/voxel-adc-se-prognosis]. While raw neuroimaging DICOMs remain restricted to uphold institutional patient privacy, the shared repository provides a comprehensive substrate for the independent verification of our prognostic inferences.

Additional information

Supplementary Information

Supplementary Table S1

Supplementary Table S2

Supplementary Table S3

Supplementary Fig. S1

Supplementary Fig. S2

Supplementary Fig. S3

Figure legends

Fig. 1. Mean voxels count distribution across ADC values in patients with status epilepticus, stratified by clinical outcome.

The blue and red lines represent patients with good and poor outcomes, respectively. ADC values are displayed on the x-axis in units of $\times 10^{-6}$ mm^2/s. The y-axis shows the average number of voxels per ADC bin, normalized across patients in each group.

Fig. 2. Distribution of normal ADC ratio across the cohort, with tertile cutoffs indicated.

Vertical dashed lines represent the 33.3rd and 66.6th percentiles, used to define Tertile 1 (low), Tertile 2 (intermediate), and Tertile 3 (high) groups.

Fig. 3. Proportion of patients with good and poor outcomes across tertile groups of the normal ADC ratio.

Good outcome rates increased across Tertile 1 to Tertile 3.

Fig. 4. Comparison of prognostic performance between voxel-based ADC metrics and clinical scores.

(A) Receiver operating characteristic (ROC) curves comparing STESS, mSTESS, the clinical-only model (age, premorbid mRS, and EEG severity), the ADC-only model using continuous normal ADC ratio, and the combined clinical–ADC model.

(B) ROC curves using dichotomized normal ADC ratio (cutoff 0.797). STESS and mSTESS demonstrated moderate discrimination, comparable to the ADC-only model, whereas combined clinical–ADC models achieved numerically higher area under the ROC curve (AUROC) values than clinical models alone. Although these improvements did not reach statistical significance, integration of voxel-based ADC metrics provided complementary prognostic information beyond established bedside scores.

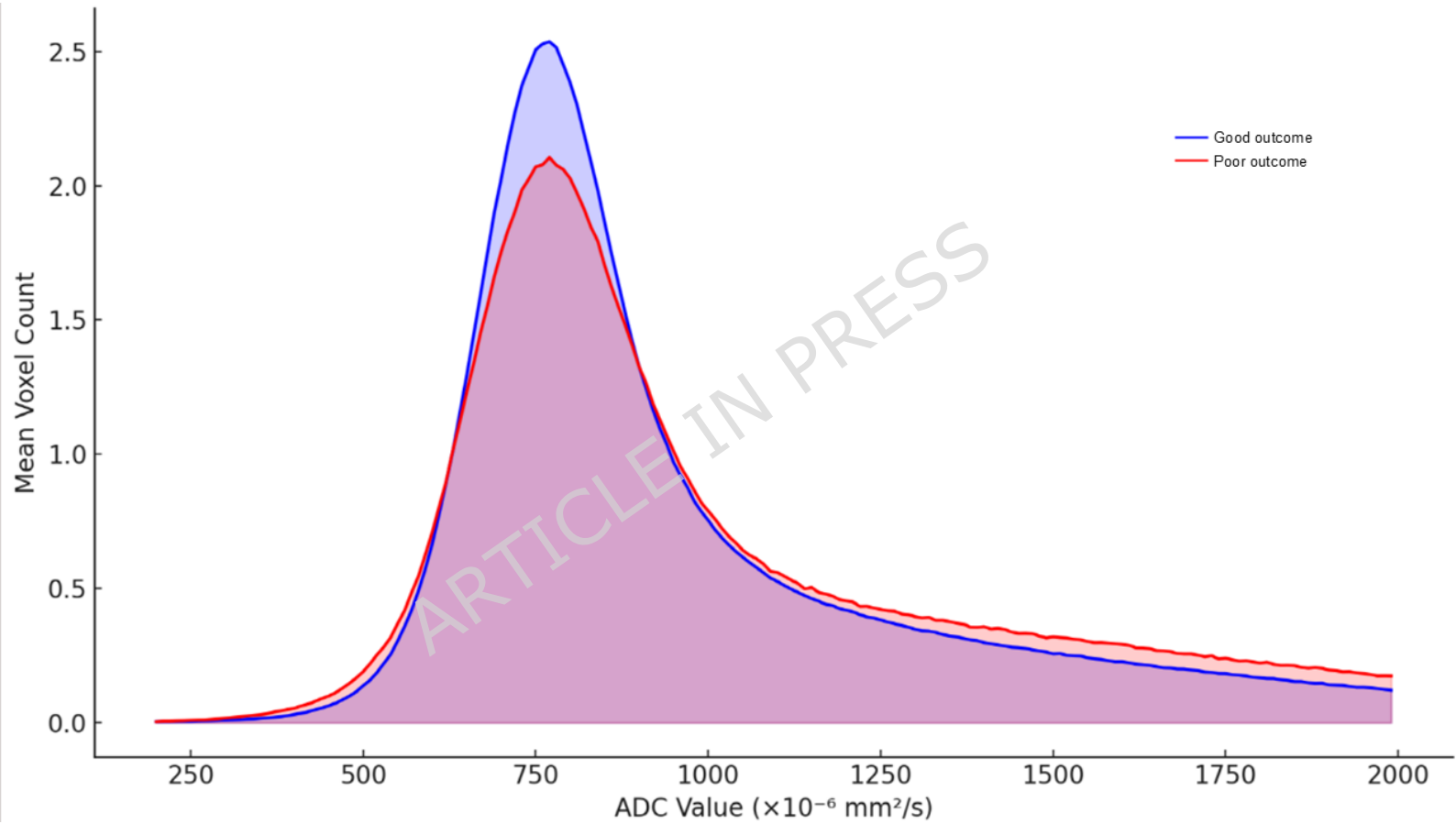

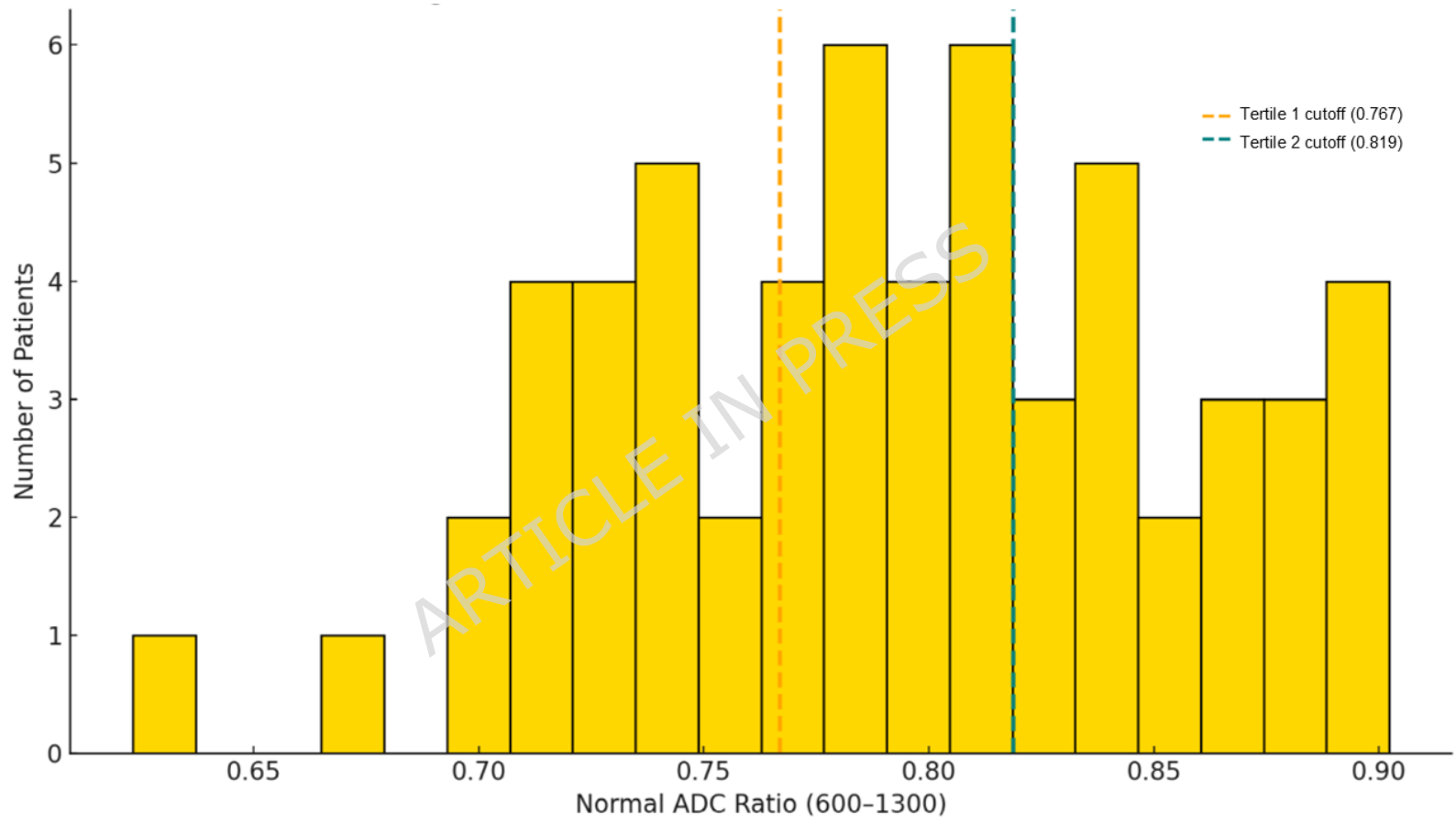

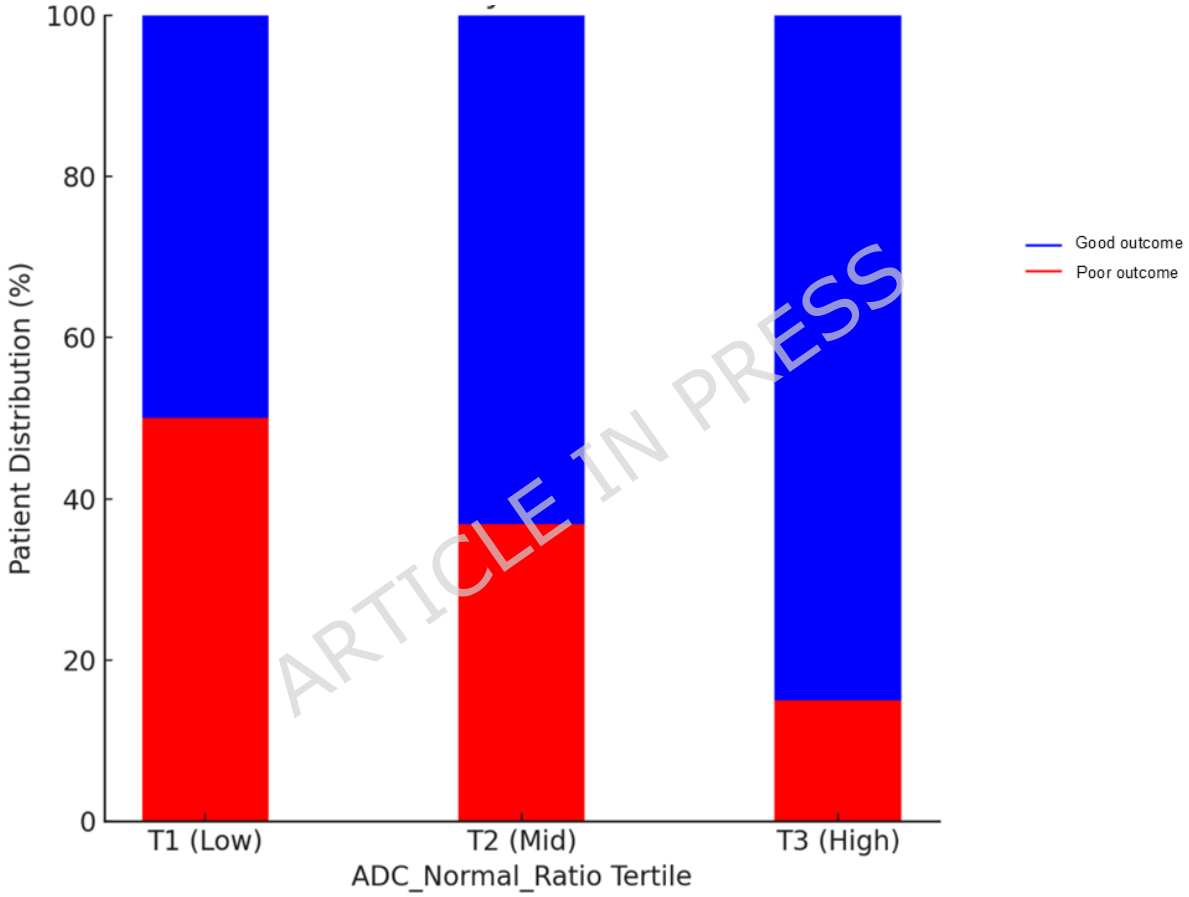

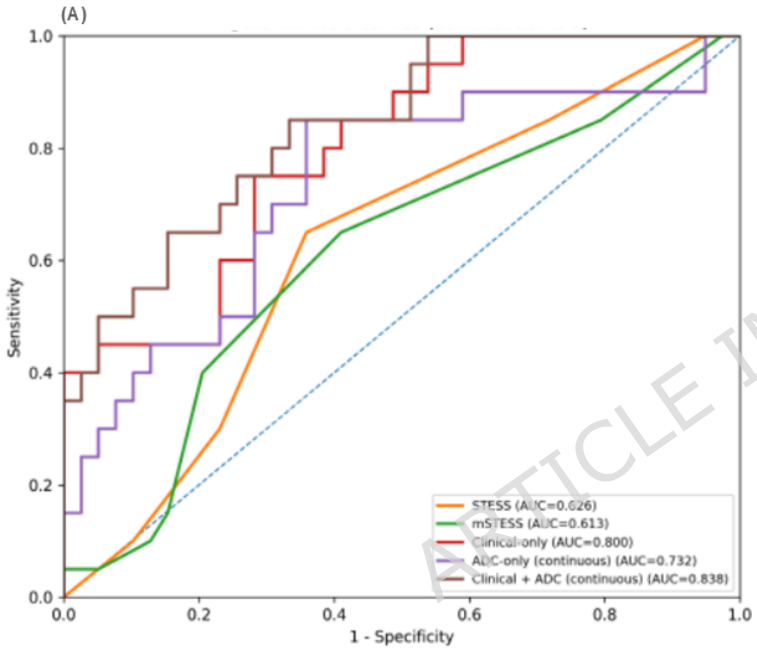

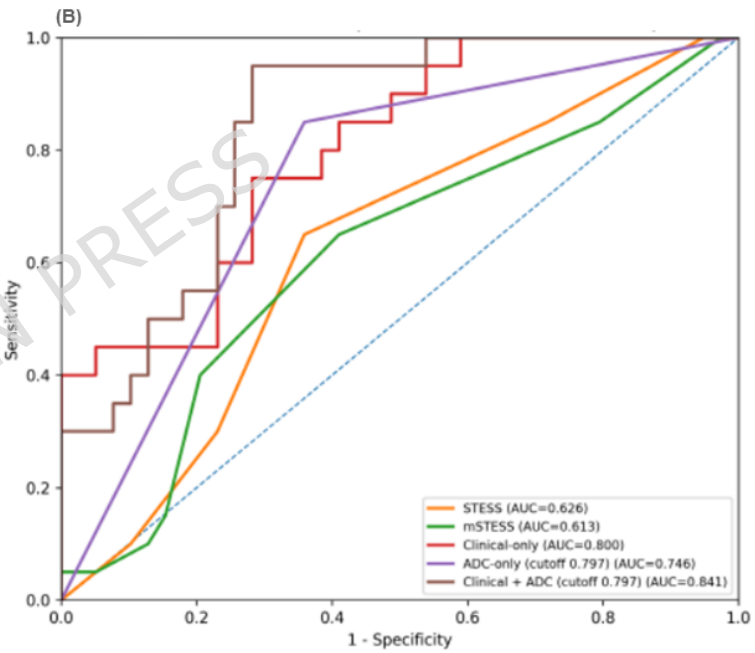

Table 1. Baseline characteristics according to clinical outcome

Variable	**Good Outcome (n= 39, 50.84%)**	**Poor Outcome (n= 20, 49.16%)**	**p-value**
Age, mean ± SD	55.9 ± 16.7	68.8 ± 16.4	0.007
Sex (male), n (%)	27 (69.2)	13 (65.0)	0.972
Diabetes mellitus, n (%)	8 (20.5)	7 (35.0)	0.371
Dyslipidemia, n (%)	6 (15.4)	2 (10.0)	0.865
Stroke, n (%)	14 (35.9)	7 (35.0)	1.000
Chronic kidney disease, n (%)	2 (5.1)	1 (5.0)	1.000
Carotid artery disease, n (%)	7 (17.9)	1 (5.0)	0.330
Cancer, n (%)	3 (7.7)	3 (15.0)	0.696
Glasgow Coma Scale, median (IQR)	8.0 (5.0–12.3)	11.0 (8.0–13.0)	0.027
SE semiology, n (%)			0.072
convulsive	30 (76.9)	10 (50.0)	
non-convulsive	9 (23.1)	10 (50.0)	
Etiology, n (%)			0.294
Acute symptomatic (structural / metabolic / toxic / infectious)	6	7	
Remote symptomatic (remote structural)	13	5	
Progressive	1	0	
Unknown	19	7	
Electroencephalography severity , n (%)			0.022

Normal	8 (20.5)	0 (0)	
Mild	9 (23.1)	2 (10.0)	
Moderate	8 (20.5)	3 (15.0)	
Severe	14 (35.9)	15 (75.0)	
Electroencephalography pattern, n (%)			0.022
No abnormality	8 (20.5)	0 (0.0)	
Diffuse slowing	9 (23.1)	2 (10.0)	
Rhythmic/focal slowing or sharp waves	8 (20.5)	3 (15.0)	
Epileptiform activity	14	5 (25.0)	
Pre-mRS, n (%)			0.858
0	17 (43.6)	10 (50.0)	
1	12 (30.8)	4 (20.0)	
2	3 (7.7)	2 (10.0)	
3	5 (12.8)	2 (10.0)	
4	2 (5.1)	2 (10.0)	
Symptom duration (min), mean ± SD	59.26 ± 70.46	139.15 ± 240.80	0.058
Proportion of normal ADC, mean ± SD	81.0 ± 5.5	75.9 ± 6.6	0.003
Time to MRI acquisition, hours, median (IQR)	6.48 (3.52–13.83)	6.10 (4.43–13.43)	0.899
ICU length of stay, days, median (IQR)	7 (3-15)	30.5 (15.8–51.3)	<0.001

ADC, apparent diffusion coefficient; mRS, modified Rankin Scale; SD, standard deviation; IQR, interquartile range

Table 2. Univariate logistic regression analysis of predictors for good functional outcome

Variable	Odds ratio (95% CI)	P-value
Age	0.95 (0.92 – 0.99)	0.011
Sex	1.21 (0.39 – 3.80)	0.742
Electroencephalography	0.36 (0.17 – 0.74)	0.006
Pre-mRS	0.97 (0.64 – 1.48)	0.889
Diabetes mellitus	0.48 (0.14 – 1.60)	0.231
Dyslipidemia	1.45 (0.39 – 5.46)	0.573
Stroke	0.91 (0.29 – 2.90)	0.878
Chronic kidney disease	0.45 (0.09 – 2.19)	0.326
Carotid artery disease	0.48 (0.14 – 1.60)	0.231
Cancer	0.48 (0.14 – 1.60)	0.231
Time to MRI acquisition (continuous MRI delay, per hour)	1.002 (0.92 – 1.09)	0.956
Time to MRI acquisition (binary MRI delay over 6h)	1.00 (0.33–3.01)	1.000

ADC_Normal_Ratio[a]	1.17 (1.02 – 1.34)	0.03
Tertile 1 (Low)	Reference	
Tertile 2 (Mid)	1.71 (0.48 – 6.16)	0.409
Tertile 3 (High)	5.67 (1.25 – 25.61)	0.024

ADC, apparent diffusion coefficient; CI, confidence intervals; mRS, modified Rankin Scale

[a]Tertile groups are based on the distribution of normal ADC ratios: Tertile 1 (0.623–0.766), Tertile 2 (0.767–0.818), and Tertile 3 (0.819–0.902).

Table 3. Multivariable logistic regression model using ROC-derived ADC threshold

Variable	**Odds ratio (95% CI)**	**P-value**
Age	0.95 (0.91 – 1.00)	0.047
Electroencephalography	0.33 (0.14 – 0.80)	0.015
Pre-mRS	1.88 (1.01 – 3.52)	0.047
Time to MRI acquisition (continuous MRI delay)	1.00 (0.91–1.11)	0.955
ADC_Group_Cutoff[†]	6.05 (1.04 – 35.09)	0.045

ADC, apparent diffusion coefficient; mRS, modified Rankin Scale; ROC, receiver operating characteristic

† ADC_Group_Cutoff refers to a dichotomized variable using a Preserved ADC cut-off of 0.797, as derived from ROC analysis (Preserved: ≥ 0.797; Non-preserved: < 0.797).